

Article

Neptunyl(VI) Nitrate Coordination Polymer with Bis(2-pyrrolidone) Linkers Highlighting Crystallographic Analogy and Solubility Difference in Actinyl(VI) Nitrates

Tomoyuki Takeyama ¹, Juliane März ², Ryoma Ono ¹, Satoru Tsushima ^{2,3} and Koichiro Takao ^{1,*}

¹ Laboratory for Zero-Carbon Energy, Institute of Innovative Research, Tokyo Institute of Technology, 2-12-1 N1-32, O-okayama, Meguro-ku, Tokyo 152-8550, Japan

² Institute of Resource Ecology, Helmholtz-Zentrum Dresden-Rossendorf, Bautzner Landstraße 400, 01328 Dresden, Germany

³ International Research Frontiers Initiative (IRFI), Institute of Innovative Research, Tokyo Institute of Technology, 2-12-1 N1-32, O-okayama, Meguro-ku, Tokyo 152-8550, Japan

* Correspondence: takao.k.ac@m.titech.ac.jp; Tel.: +81-3-5734-2968

Abstract: $\text{NpO}_2(\text{NO}_3)_2$ units are connected by bis(2-pyrrolidone) linker molecules with the *trans*-1,4-cyclohexyl bridging part (**L1**) to form a one-dimensional coordination polymer, $[\text{NpO}_2(\text{NO}_3)_2(\text{L1})]_n$. Molecular and crystal structures of this compound are nearly identical to that of the UO_2^{2+} analogue, while its aqueous solubility is greatly enhanced, probably owing to weaker thermodynamic stability of the complexation in NpO_2^{2+} compared with that in UO_2^{2+} .

Keywords: coordination polymer; actinides; neptunium; crystallography; solubility; nuclear fuel recycling



Citation: Takeyama, T.; März, J.; Ono, R.; Tsushima, S.; Takao, K. Neptunyl(VI) Nitrate Coordination Polymer with Bis(2-pyrrolidone) Linkers Highlighting Crystallographic Analogy and Solubility Difference in Actinyl(VI) Nitrates. *Inorganics* **2023**, *11*, 104. <https://doi.org/10.3390/inorganics11030104>

Academic Editor: Wolfgang Linert

Received: 6 February 2023

Revised: 25 February 2023

Accepted: 27 February 2023

Published: 1 March 2023



Copyright: © 2023 by the authors. Licensee MDPI, Basel, Switzerland. This article is an open access article distributed under the terms and conditions of the Creative Commons Attribution (CC BY) license (<https://creativecommons.org/licenses/by/4.0/>).

1. Introduction

In nuclear fuel recycling, spent nuclear fuels are dissolved in $\text{HNO}_3(\text{aq})$, and then subjected to separation and purification of fissile materials such as U and Pu. This process is called *reprocessing*, and constitutes one of the most important steps in the nuclear fuel cycle [1]. While the *plutonium uranium redox extraction* (PUREX) process, based on solvent extraction, is well-known as a standard approach for this purpose, a variety of other reprocessing methods based on wet chemical and pyrochemical bases have also been proposed. Our group is also developing a new precipitation-based reprocessing called *nuclear fuel materials selective precipitation*, NUMAP [2], where *N*-alkylated 2-pyrrolidone derivatives (NRPs, Figure 1) are employed for efficient and simultaneous precipitation of U and Pu from $\text{HNO}_3(\text{aq})$ [3,4]. In the NUMAP approach, Pu will be deliberately recovered together with U for the sake of securing nuclear proliferation resistivity. This is in strong contrast to PUREX, which has been developed to isolate Pu for nuclear weapons. Similar precipitation-based reprocessing concepts are also proposed by other groups [5,6].

Understanding the coordination chemistry of early actinides with NO_3^- as well as with selected ligands like NRPs is highly essential to establish foundations of chemical separation in any wet chemical reprocessing processes. The early actinides such as U, Np, and Pu exhibit rich redox chemistry, with common oxidation states varying between III and VI [7]. In penta- and hexavalent states, actinyl ions (AnO_2^{m+} ; An = U, Np, Pu; $m = 1, 2$) are formed, where the equatorial plane is offered for additional coordination of extra ligands, as exemplified by $\text{AnO}_2(\text{NO}_3)_2(\text{NRP})_2$ in Figure 1. By exploiting such uniqueness in coordination chemistry, we extended the molecular design of NRPs to double-headed ones, DHNRPs (Figure 1), to form a much less-soluble $[\text{UO}_2(\text{NO}_3)_2(\text{DHNRP})]_n$ coordination polymer to further improve the recovery efficiency of UO_2^{2+} precipitate [8–10].

In the reprocessing process, Pu is intended to be recovered together with UO_2^{2+} , whereas Np should be removed from them. In the first phase of NUMAP development,

hydrophobic NRP-like NCP (Figure 1) has been preferably employed to achieve high recovery yields of UO_2^{2+} and PuO_2^{2+} [4,11–14]. Therefore, we are now strongly motivated to explore how NpO_2^{2+} and PuO_2^{2+} , the heavier analogues of UO_2^{2+} , react with DHNRPs in $\text{HNO}_3(\text{aq})$. While the stability of hexavalent states of Np and Pu are generally decreasing, more common oxidation numbers for them are V and IV, respectively. Nevertheless, we are still interested in determining the coordination behavior of the AnO_2^{2+} family with DHNRPs, through which chemical analogy may be observed. Accordingly, it is valuable to first gain knowledge about what happens on NpO_2^{2+} , which is only allowed to be handled in a dedicated facility, in order to judge whether or not it is worth studying PuO_2^{2+} in this direction. Herein, we have assessed the structural chemistry of an NpO_2^{2+} coordination polymer with NO_3^- and DHNRPs (**L1**, *rac*-**L2**), as well as its solubility, in 3 M $\text{HNO}_3(\text{aq})$, typically used in the reprocessing process.

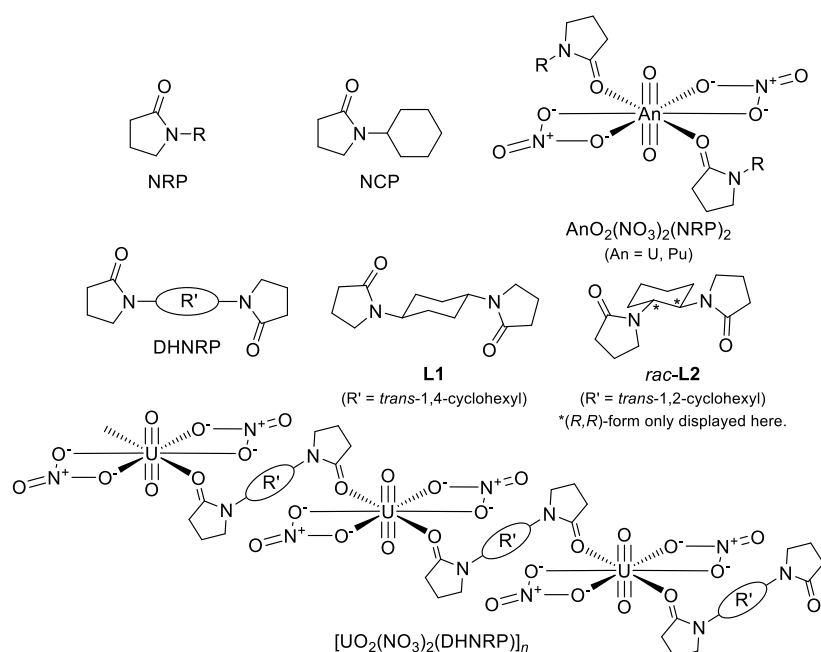


Figure 1. Schematic structures of NRPs, DHNRPs, and their actinyl(VI) nitrate complexes.

2. Results and Discussion

A 3 M HNO_3 solution dissolving 100 mM NpO_2^{2+} (25 μL) was layered with a blank 3 M $\text{HNO}_3(\text{aq})$ (50 μL) and that containing 200 mM **L1** (12.5 μL) from bottom to top in a glass tube ($\phi 5$ mm) inserted into a 2 mL glass vial, where $\text{NpO}_2^{2+}:\text{L1} = 1:1$. This layered mixture was stored in a silent place overnight in a glovebox dedicated for Np experiments. Through natural diffusion of the components in the solution phase, yellowish-brown crystals suitable for X-ray crystallography deposited, as shown in Figure 2. A γ -ray spectrometry of the supernatant allowed to know that this crystalline deposit contained Np and that its yield was 44% based on the initial loading of NpO_2^{2+} .

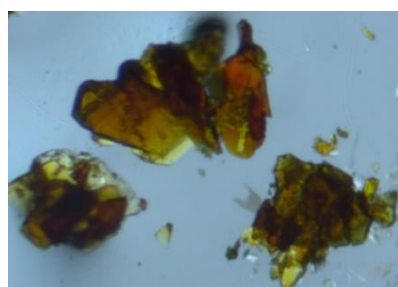


Figure 2. Photomicrograph of deposited crystals of $[\text{NpO}_2(\text{NO}_3)_2(\text{L1})]_n$.

Molecular and crystal structures of this compound were determined by single crystal X-ray analysis at 293 K. As a result, this compound shown in Figure 3 was found to consist of $\text{NpO}_2(\text{NO}_3)_2$ units connected by **L1** linker molecules to form an infinite one-dimensional (1D) coordination polymer, $[\text{NpO}_2(\text{NO}_3)_2(\text{L1})]_n$, which should be formed through the following reaction in the HNO_3 solution.



While we have mentioned above that Np exhibits a wide variety of oxidation numbers from III to VI, or even to VII, as one of unique trends of early actinide elements [7,15,16], its hexavalent oxidation state remained unchanged in the current system.

Crystallographic data of $[\text{NpO}_2(\text{NO}_3)_2(\text{L1})]_n$ are summarized in Table 1. This coordination polymer crystallized in triclinic $P-1$ with $a = 6.0172(2) \text{ \AA}$, $b = 7.6661(2) \text{ \AA}$, $c = 11.0985(3) \text{ \AA}$, $\alpha = 75.9330(10)^\circ$, $\beta = 84.488(2)^\circ$, and $\gamma = 76.353(2)^\circ$. A volume of its unit cell (V) was $482.18(2) \text{ \AA}^3$. As shown in this table, all of the crystallographic data of the current compound are almost identical to those of its UO_2^{2+} analogue, $[\text{UO}_2(\text{NO}_3)_2(\text{L1})]_n$ (triclinic $P-1$, $a = 5.8962(4) \text{ \AA}$, $b = 7.6330(6) \text{ \AA}$, $c = 11.0279(9) \text{ \AA}$, $\alpha = 76.841(5)^\circ$, $\beta = 84.480(6)^\circ$, $\gamma = 76.229(5)^\circ$, and $V = 468.93(6) \text{ \AA}^3$), we reported previously [9]. Both UO_2^{2+} and NpO_2^{2+} form isomorphous crystalline phases of $[\text{AnO}_2(\text{NO}_3)_2(\text{L1})]_n$ because of the chemical similarity of AnO_2^{2+} ions.

Table 1. Crystallographic data of $[\text{AnO}_2(\text{NO}_3)_2(\text{L1})]_n$ (An = Np, U).

	$[\text{NpO}_2(\text{NO}_3)_2(\text{L1})]_n$	$[\text{UO}_2(\text{NO}_3)_2(\text{L1})]_n$
formula	$\text{C}_{14}\text{H}_{22}\text{N}_4\text{NpO}_{10}$	$\text{C}_{14}\text{H}_{22}\text{N}_4\text{O}_{10}\text{U}$
F_w	643.35	644.38
system	triclinic	triclinic
space group	$P-1$ (#2)	$P-1$ (#2)
crystal size/ mm^3	$0.22 \times 0.09 \times 0.04$	$0.400 \times 0.300 \times 0.200$
$a/\text{\AA}$	6.0172(2)	5.8962(4)
$b/\text{\AA}$	7.6661(2)	7.6330(6)
$c/\text{\AA}$	11.0985(3)	11.0279(9)
$\alpha/^\circ$	75.9330(10)	76.841(5)
$\beta/^\circ$	84.488(2)	84.480(6)
$\gamma/^\circ$	76.353(2)	76.229(5)
$V/\text{\AA}^3$	482.18(2)	468.93(6)
Z	1	1
T/K	293	93
$D_{\text{calc}}/\text{g}\cdot\text{cm}^{-3}$	2.216	2.282
$\mu(\text{Mo K}\alpha)/\text{mm}^{-1}$	5.450	8.720
R_1 ($I > 2\sigma$)	0.0284	0.0174
wR_2 (all)	0.0512	0.0393
GOF	1.173	1.042
CCDC No.	2208277	1573161
ref.	this work	[9]

As shown in Figure 3, the central Np atom is surrounded by two axial O atoms of NpO_2^{2+} (O_{ax}) and by six equatorial O atoms of two bidentate NO_3^- ions (O_{NO_3}) and two monodentate 2-pyrrolidone moieties of the different **L1** molecules (O_{L}) to afford a hexagonal bipyramidal coordination polyhedron. The asymmetric unit comprises only one Np, one O_{ax} , one NO_3^- , and half of **L1**, which is expanded by an inversion center (symmetry operation: (i) $1 - x, 1 - y, -z$) to complete a whole structure of the $[\text{NpO}_2(\text{NO}_3)_2(\text{L1})]_n$ monomer. As a result, these sets of ligands are located at *trans*-positions, which is rather ordinarily found in actinyl(VI) nitrates, as reviewed elsewhere [17,18].

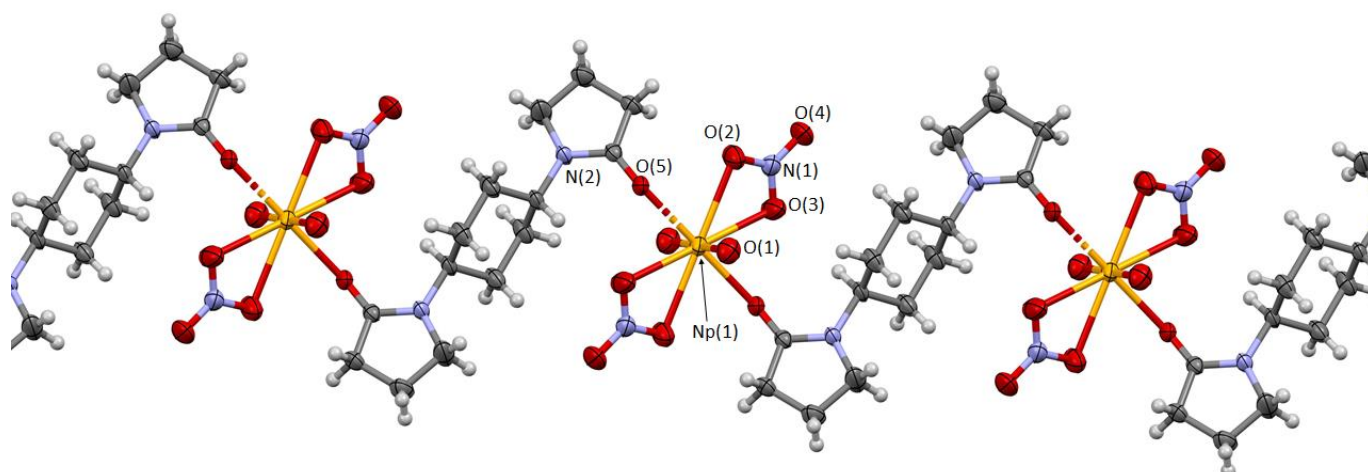


Figure 3. ORTEP view of $[\text{NpO}_2(\text{NO}_3)_2(\text{L1})]_n$ at the 50% probability level. Crystallographic data on $[\text{NpO}_2(\text{NO}_3)_2(\text{L1})]_n$: CCDC 2208277, $\text{C}_{14}\text{H}_{22}\text{N}_4\text{Np}_1\text{O}_{10}$, $F_w = 643.35$, $0.22 \times 0.09 \times 0.04 \text{ mm}^3$, triclinic, $P\bar{1}$, $a = 6.0172(2) \text{ \AA}$, $b = 7.6661(2) \text{ \AA}$, $c = 11.0985(3) \text{ \AA}$, $\alpha = 75.9330(10)^\circ$, $\beta = 84.488(2)^\circ$, $\gamma = 76.353(2)^\circ$, $V = 482.18(2) \text{ \AA}^3$, $Z = 1$, $T = 293 \text{ K}$, $D_{\text{calcd}} = 2.216 \text{ g/cm}^3$, $\mu(\text{Mo K}\alpha) = 5.450 \text{ mm}^{-1}$, $GOF = 1.173$, $R_1(I > 2\sigma) = 0.0284$, $wR_2(\text{all}) = 0.0512$.

Selected structural parameters of $[\text{NpO}_2(\text{NO}_3)_2(\text{L1})]_n$ were summarized in Table 2 together with those of $[\text{UO}_2(\text{NO}_3)_2(\text{L1})]_n$ [9]. The $\text{Np}\equiv\text{O}_{\text{ax}}$ bond length ($\text{Np}(1)\text{--O}(1)$) is $1.744(3) \text{ \AA}$, while longer distances can be found in $\text{Np}\text{--O}_{\text{NO}_3}$ ($\text{Np}\text{--O}(2)$, $\text{Np}\text{--O}(3)$): mean 2.56 \AA and $\text{Np}\text{--O}_{\text{L}}$ ($\text{Np}\text{--O}(5)$: $2.341(2) \text{ \AA}$) interactions formed in the equatorial plane. The $\text{O}_{\text{ax}}\equiv\text{Np}\equiv\text{O}_{\text{ax}}$ bond angle in NpO_2^{2+} is exactly 180° owing to its centrosymmetric structure in this compound. These structural data are common to those observed in $\text{NpO}_2(\text{NO}_3)_2(\text{OPPh}_3)_2$ ($\text{Np}\equiv\text{O}_{\text{ax}}$: $1.739(10) \text{ \AA}$, $\text{Np}\text{--O}_{\text{NO}_3}$: 2.53 \AA (mean), $\text{Np}\text{--O}_{\text{OPPh}_3}$: $2.363(8) \text{ \AA}$), which is a *trans*-dinitrato NpO_2^{2+} complex with two monodentate ligands solely known so far [19]. There are several related structures in which the equatorial coordination is constrained in a *cis*-geometry by additional bidentate ligands, such as 2,2'-bipyridyl (bpy) and $\text{BrCH}_2\text{COO}^-$, or by dimerization through two $\mu\text{-OH}^-$ bridges [20–22]. Regardless of such *cis-trans* isomerization, the $\text{Np}\equiv\text{O}_{\text{ax}}$ distance of the current compound ($1.739(10) \text{ \AA}$) is not very different from the reported *cis*-structures ($1.73\text{--}1.76 \text{ \AA}$). In contrast, it seems to be difficult to directly compare the $\text{Np}\text{--O}_{\text{NO}_3}$ interactions in $[\text{NpO}_2(\text{NO}_3)_2(\text{L1})]_n$ in the *trans*-geometry (mean: 2.53 \AA) to those in the known *cis*-complexes owing to the wider variety in $\text{Np}\text{--O}_{\text{NO}_3}$ lengths of the latter series from 2.47 \AA to 2.56 \AA .

Table 2. Selected structural parameters of $[\text{AnO}_2(\text{NO}_3)_2(\text{L1})]_n$.

	$\text{An} = \text{Np}^a$	$\text{An} = \text{U}^b$
	bond distance (\AA)	
$\text{An}\text{--O}_{\text{ax}}$	$\text{Np}\text{--O}(1)$ 1.744(3)	1.769(2)
$\text{An}\text{--O}_{\text{NO}_3}$	$\text{Np}\text{--O}(2)$ 2.551(3)	2.546(2)
	$\text{Np}\text{--O}(3)$ 2.562(3)	2.550(2)
$\text{An}\text{--O}_{\text{L}}$	$\text{Np}\text{--O}(5)$ 2.341(2)	2.362(2)
$\text{C}_{\text{carb}} = \text{O}_{\text{L}}$	$\text{C}(1)\text{--O}(5)$ 1.254(4)	1.260(4)
$\text{C}_{\text{carb}}\text{--N}_{\text{amide}}$	$\text{C}(1)\text{--N}(2)$ 1.325(4)	1.329(4)
	bond angles ($^\circ$)	
$\text{O}_{\text{ax}}\equiv\text{An}\equiv\text{O}_{\text{ax}}$	$\text{O}(1)\text{--Np}(1)\text{--O}(1)^i$ 180	180
$\text{An}\text{--O}_{\text{L}} = \text{C}$	$\text{Np}(1)\text{--O}(5)\text{--C}(1)$ 138.3(2)	134.4(2)
	tilt angles from AnO_2^{2+} equatorial plane ($^\circ$)	
NO_3^-	13.8	12.3
2-pyrrolidone	43.0	46.6

^a This work at 293 K. Atomic notations follow Figure 3. Symmetry operation: (i) $1 - x, 1 - y, -z$. ^b [9] at 93 K.

As shown in Table 2, $[\text{NpO}_2(\text{NO}_3)_2(\text{L1})]_n$ is isostructural with $[\text{UO}_2(\text{NO}_3)_2(\text{L1})]_n$ in terms of molecular structure as well, where the contribution of the actinide contraction is not clearly observed. Charushnikova et al. reported a molecular structure of $[\text{N}(\text{CH}_3)_4][\text{Np}^{\text{V}}\text{O}_2(\text{NO}_3)_2(\text{H}_2\text{O})_2]$, where Np is pentavalent [23]. Although the coordination geometry around its Np^{5+} center was also hexagonal bipyramidal in a similar manner to the current compound, the bond distances of this Np(V) complex ($\text{Np}\equiv\text{O}_{\text{ax}}$: 1.823(1) Å, $\text{Np}-\text{O}_{\text{NO}_3}$: 2.62 Å (mean), $\text{Np}-\text{O}_{\text{H}_2\text{O}}$: 2.473(1) Å) are critically different from those in Table 2. The significantly shorter interactions around the Np center of $[\text{NpO}_2(\text{NO}_3)_2(\text{L1})]_n$ reported here indicate that its hexavalence is maintained.

Each crystal lattice of this compound contains a $[\text{NpO}_2(\text{NO}_3)_2(\text{L1})]$ monomer, which polymerizes along the *c*-axis (Figures 3, Figure 4 and S1). In the directions of *a*- and *b*-axes, the $[\text{NpO}_2(\text{NO}_3)_2(\text{L1})]_n$ coordination polymers stack each other through $\text{C}-\text{H}\cdots\text{O}$ interactions between the independent 1D chains ($D\cdots A$: $\text{C}\cdots\text{O}_{\text{ax}}$ = 3.46–3.55 Å, $\text{C}\cdots\text{O}_{\text{NO}_3}$ = 3.28–3.63 Å, $\text{C}\cdots\text{O}_{\text{L}}$ = 3.61–3.65 Å; $D-H\cdots A$: $\text{C}-\text{H}\cdots\text{O}_{\text{ax}}$ = 2.58–2.60 Å, $\text{C}-\text{H}\cdots\text{O}_{\text{NO}_3}$ = 2.42–2.70 Å, $\text{C}-\text{H}\cdots\text{O}_{\text{L}}$ = 2.68–2.69 Å). These packing trends are also common to those of $[\text{UO}_2(\text{NO}_3)_2(\text{L1})]_n$ [9].

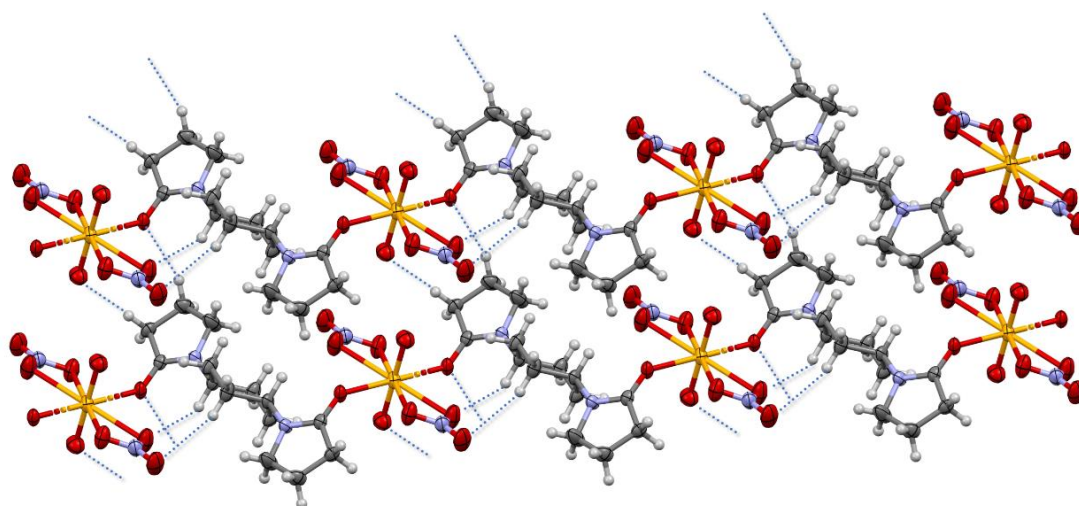


Figure 4. $\text{C}-\text{H}\cdots\text{O}$ interactions occurring in the crystal structure of $[\text{NpO}_2(\text{NO}_3)_2(\text{L1})]_n$. Although more interactions can be found there, only some of them are drawn with dotted lines here for clarity. Color codes, Np: yellow, O: red, N: purple, C: grey, H: white.

Previously, we defined a mean volume of one C atom of an alkyl group (R, Figure 1) of NRPs as a compactness parameter (C_P , Å³) as follows [12].

$$C_P = (V/Z - V_0/Z_0)/2N_C, \quad (2)$$

where V and Z are the cell volume and the number of $\text{UO}_2(\text{NO}_3)_2(\text{NRP})_2$ units in a crystal lattice, respectively. The subscript “0” indicates those of $\text{UO}_2(\text{NO}_3)_2(2\text{-pyrrolidone})_2$, where NRP with $\text{R} = \text{H}$ (Figure 1) is employed. N_C is the number of C atoms in R. C_P can be compared as a measure of packing efficiency of $\text{UO}_2(\text{NO}_3)_2(\text{NRP})_2$, and is an important factor to govern the solubility of UO_2^{2+} in $\text{HNO}_3(\text{aq})$, i.e., recovery yield of U in our NUMAP reprocessing for the nuclear fuel recycling. Thereafter, this concept was expanded to the coordination polymers of $[\text{UO}_2(\text{NO}_3)_2(\text{DHNRP})]_n$, where half of the number of C atoms in R’ of DHNRP (Figure 1) was taken as N_C owing to its stoichiometric ratio [2,9]. Based on the structural similarity with the UO_2^{2+} analogue discussed above, C_P of $[\text{NpO}_2(\text{NO}_3)_2(\text{L1})]_n$ was calculated to be 16.4 Å³ ($V_0/Z_0 = 383.9$ Å³ at 293 K) [9]. This is slightly greater than that of $[\text{UO}_2(\text{NO}_3)_2(\text{L1})]_n$ ($C_P = 15.6$ Å³), but still much smaller than those of $\text{UO}_2(\text{NO}_3)_2(\text{NRP})_2$ complexes ($C_P = 20.4 - 30.3$ Å³). Therefore, the higher packing efficiency of $\text{NpO}_2(\text{NO}_3)_2$ units is still maintained in $[\text{NpO}_2(\text{NO}_3)_2(\text{L1})]_n$.

Up to now, we have not found any significant differences arising from variation in the hexavalent actinide center of $[\text{AnO}_2(\text{NO}_3)_2(\mathbf{L1})]_n$ from the viewpoint of structural chemistry. Seemingly, such a similarity might allow us to anticipate co-crystallization of any AnO_2^{2+} ions from $\text{HNO}_3(\text{aq})$ after loading $\mathbf{L1}$ to form the heterometallic 1D coordination polymer. Nevertheless, we should reject this expectation, because the recovery yield of NpO_2^{2+} from 3 M $\text{HNO}_3(\text{aq})$ was only 44% after loading an equimolar amount of $\mathbf{L1}$ at 293 K, as described above. This means that the solubility of $[\text{NpO}_2(\text{NO}_3)_2(\mathbf{L1})]_n$ is 16 mM under this condition, which is one order of magnitude higher than that of $[\text{UO}_2(\text{NO}_3)_2(\mathbf{L1})]_n$ (2.48 mM) [9]. It is rather close to that of $\text{UO}_2(\text{NO}_3)_2(\text{NRP})_2$ (R = cyclohexyl, 17.6 mM, $C_p = 21.4 \text{ \AA}^3$) [2]. Here, we found a uniqueness of NpO_2^{2+} .

As mentioned above, the structural features cannot explain this gap. We wonder whether the difference in solubility of $[\text{AnO}_2(\text{NO}_3)_2(\mathbf{L1})]_n$ between An = U and Np could be ascribed to the thermodynamic stability of the complexation around AnO_2^{2+} . Indeed, stability constants ($\log \beta$) of AnO_2^{2+} complexes in several ligand systems (CO_3^{2-} , CH_3COO^- , F^-) sequentially decrease with an increase in the atomic number of the center metal, as summarized in Table S1 [16,24]. We are also aware that such a trend is not always clear for other weaker ligands (Cl^- , SO_4^{2-}), and that $\log \beta$ of NO_3^- is only available for UO_2^{2+} despite the highest relevance to the current work. Although it is still difficult to know exactly why the solubility of $[\text{NpO}_2(\text{NO}_3)_2(\mathbf{L1})]_n$ is unexpectedly higher than the UO_2^{2+} analogue, this knowledge provides an important implication to consider the recovery of PuO_2^{2+} using $\mathbf{L1}$ from $\text{HNO}_3(\text{aq})$ in our NUMAP reprocessing for nuclear fuel recycling [2].

Using *rac*- $\mathbf{L2}$ (see Figure 1), we previously confirmed that $[\text{UO}_2(\text{NO}_3)_2(\textit{rac}\text{-}\mathbf{L2})]_n$ deposited from 3 M $\text{HNO}_3(\text{aq})$ [9]. Therefore, we examined what happens in a mixture of NpO_2^{2+} with *rac*- $\mathbf{L2}$ as follows. The aqueous solution with 3 M HNO_3 and 100 mM NpO_2^{2+} (25 μL) was placed at the bottom of the $\phi 5$ mm glass tube, followed by subsequent loading of a blank 3 M $\text{HNO}_3(\text{aq})$ (50 μL) and that dissolving 200 mM *rac*- $\mathbf{L2}$ (12.5 μL), where NpO_2^{2+} : *rac*- $\mathbf{L2}$ = 1:1. Finally, nothing deposited even after several days passed. However, this result is not very surprising, because we have already known that *rac*- $\mathbf{L2}$ affords a more soluble coordination polymer of $[\text{UO}_2(\text{NO}_3)_2(\textit{rac}\text{-}\mathbf{L2})]_n$ (14.8 mM) compared with $[\text{UO}_2(\text{NO}_3)_2(\mathbf{L1})]_n$ (2.48 mM) [9]. Accordingly, the solubility of the NpO_2^{2+} analogue with *rac*- $\mathbf{L2}$ would also be higher than that of $\mathbf{L1}$ described above (16 mM). When the sample solution was fully mixed, the total concentration of NpO_2^{2+} was 28.6 mM. While there are no reasons to exclude the possibility of formation of the $[\text{NpO}_2(\text{NO}_3)_2(\textit{rac}\text{-}\mathbf{L2})]_n$ coordination polymer in a similar manner to $[\text{UO}_2(\text{NO}_3)_2(\textit{rac}\text{-}\mathbf{L2})]_n$, its solubility in 3 M $\text{HNO}_3(\text{aq})$ would be higher than 28.6 mM, the total concentration of NpO_2^{2+} loaded to the reaction mixture of the current experimental runs.

3. Conclusions

In this paper, we have succeeded in the synthesis and structure determination of the NpO_2^{2+} coordination polymer, $[\text{NpO}_2(\text{NO}_3)_2(\mathbf{L1})]_n$. While its molecular and crystal structures are nearly identical to those of the UO_2^{2+} analogue, a significant difference in aqueous solubility was observed between them. At this moment, we suppose that it is related to the thermodynamic stability of the formed complexes. Although there are only two cases of UO_2^{2+} and NpO_2^{2+} , such a trend would be extendable to PuO_2^{2+} . If so, the solubility of $[\text{PuO}_2(\text{NO}_3)_2(\mathbf{L1})]_n$ should be too high to recover PuO_2^{2+} efficiently from the HNO_3 feed solution dissolving the spent nuclear fuels. Furthermore, deposition of $[\text{NpO}_2(\text{NO}_3)_2(\textit{rac}\text{-}\mathbf{L2})]_n$ was unsuccessful, most probably because of its higher solubility compared with that of $[\text{NpO}_2(\text{NO}_3)_2(\mathbf{L1})]_n$. This trend in solubility would be predicted to be enhanced with an increase in the atomic number. Therefore, recovery of Pu as PuO_2^{2+} using DHNRP will be less expectable.

In contrast, we have recently succeeded in the preparation of An^{4+} compounds with $\mathbf{L1}$ or *rac*- $\mathbf{L2}$ from $\text{HNO}_3(\text{aq})$, where $[\text{An}(\text{NO}_3)_6]^{2-}$ (An = Th, U, Np) forms a sparingly soluble salt with anhydrous H^+ counteranions polymerized through hydrogen bonds with these DHNRPs [10,25,26]. The solubility of $(\text{HDHNR})_2[\text{An}(\text{NO}_3)_6]$ is only several millimolars,

regardless of the difference in An^{4+} tested so far, where there is little periodic trend, unlike that of AnO_2^{2+} found in this work. In conclusion, it would be better to anticipate the recovery of Pu in its tetravalent form, Pu^{4+} , which is the most common oxidation state of Pu in the feed solution after dissolution of the spent nuclear fuels in $\text{HNO}_3(\text{aq})$. Accordingly, our next task is to examine whether or not Pu^{4+} indeed forms $(\text{HDHNR})_2[\text{Pu}(\text{NO}_3)_6]$ with solubility low enough for its recovery in nuclear fuel recycling.

4. Experimental

4.1. Materials

Caution! ^{237}Np is a radioactive isotope emitting alpha radiation (specific activity: $2.63 \times 10^7 \text{ Bq g}^{-1}$ with $T_{1/2} = 2.14 \times 10^6$ years). It has to be handled in dedicated facilities with appropriate equipment for radioactive materials to avoid health risks caused by radiation exposure. All of the operations in handling Np were performed in a dedicated glove box in the control area of HZDR. Furthermore, HNO_3 used in this work should be used under great caution for chemical safety because of its strong acidity and oxidizing nature.

All reagents used were of reagent grade and used as received, if not specified. The **L1** and *rac*-**L2** ligands were synthesized as described below [9]. Neptunyl(VI) nitrate hydrate ($\text{Np}^{\text{VI}}\text{O}_2(\text{NO}_3)_2 \cdot n\text{H}_2\text{O}$, $n \sim 5$) was prepared by dissolving NpO_2 (29.8 mg, 0.111 mmol) in conc. HNO_3 (aq.). This solution was refluxed for two days and concentrated to near to dryness on a hot plate. The final residue of $\text{Np}^{\text{VI}}\text{O}_2(\text{NO}_3)_2 \cdot n\text{H}_2\text{O}$ was dissolved in 1.11 mL of 3 M HNO_3 (aq.) to prepare 100 mM $\text{Np}^{\text{VI}}\text{O}_2(\text{NO}_3)_2$ with 3 M HNO_3 stock solution. The concentration of NpO_2^{2+} was determined by the γ -ray spectrometry.

4.2. Synthesis of **L1**

In a 200 mL round bottom flask, *trans*-1,4-cyclohexanediamine (1.225 g, 10.73 mmol, TCI), K_2CO_3 (6.10 g, 44.2 mmol, Wako), and THF (80 mL, Wako) were loaded. Under cooling on an ice bath and vigorous stirring, 4-chlorobutyl chloride (2.45 mL, 3.09 g, 21.90 mmol, TCI) was slowly added through a dropping funnel. This mixture was stirred at 0 °C for 2 h, and then further reacted at room temperature overnight. After removal of the solvent by evaporation under reduced pressure, water (70 mL) was loaded to the residue, followed by sonication and stirring at room temperature. The colorless insoluble solid was recovered by filtration, washed with H_2O several times, and dried under vacuum to obtain *N,N'*-*trans*-cyclohexane-1,4-diylbis(4-chlorobutanamide) (2.50 g, 72% yield). ^1H NMR (δ/ppm vs. TMS, CDCl_3 , 399.78 MHz) 5.47 (NH, bs, 2H), 3.76 (N- CH_{ax} , br, 2H), 3.58 (CH_2Cl , t, 4H), 2.33 (CH_2 , t, 4H), 2.11 (CH_2 , quintet, 4H), 2.01 (CH_{eq} , d, 4H), 1.27 (CH_{ax} , td, 4H). ^{13}C NMR (δ/ppm vs. TMS, CDCl_3 , 100.53 MHz) 171.03, 47.71, 44.67, 33.50, 31.79, 28.22.

This precursor (2.42 g, 7.44 mmol) was loaded in a 200 mL round bottom flask together with CH_2Cl_2 (70 mL), followed by cooling on the ice bath. To this solution, potassium *tert*-butoxide (1.85 g, 16.5 mmol) dissolved in THF (40 mL) was slowly added through a dropping funnel. The reaction mixture was stirred at 0 °C overnight. After passing through a Celite pad, the filtrate was concentrated by a rotary evaporator. Adding hexane (40 mL) to the residual oil under sonication allowed to form a colorless solid, which was recovered by suction filtration and dried under vacuum to obtain **L1** (1.54 g) in 83% yield. ^1H NMR (δ/ppm vs. TMS, CDCl_3 , 399.78 MHz) 3.97 (N- CH_{ax} , br, 2H), 3.33 (CH_2 , t, 4H), 2.39 (CH_2 , t, 4H), 2.00 (CH_2 , quintet, 4H), 1.77 (CH_{eq} , d, 4H), 1.60 (CH_{ax} , td, 4H). ^{13}C NMR (δ/ppm vs. TMS, CDCl_3 , 100.53 MHz) 171.03, 47.71, 44.67, 33.50, 31.79, 28.22.

4.3. Synthesis of *rac*-**L2**

In a 500 mL round bottom flask, *trans*-1,2-cyclohexanediamine (5.08 g, 44.4 mmol, TCI), triethylamine (8.99 g, 88.8 mmol, Kanto), and THF (200 mL, Wako) were loaded. Under cooling on an ice bath and vigorous stirring, 4-chlorobutyl chloride (9.95 mL, 12.5 g, 88.9 mmol, TCI) was slowly added through a dropping funnel. This mixture was stirred at 0 °C for 2 h, and then further reacted at room temperature overnight. After filtration

of the reaction mixture, the obtained solid was dispersed in H₂O (150 mL). The insoluble colorless solid was recovered by filtration, washed with H₂O several times, and dried under vacuum to obtain *N,N'*-*trans*-cyclohexane-1,2-diylbis(4-chlorobutanamide) (6.58 g, 46% yield). The filtrate after the reaction was concentrated by the rotary evaporator. To the residue, CH₂Cl₂ (130 mL) and 2 M HCl aq (10 mL) were loaded, followed by vigorous stirring of this mixture. The organic layer was separated from the aqueous phase and mixed with K₂CO₃ and MgSO₄. The separated supernatant was concentrated and triturated with cold hexane (100 mL) in the ice bath. The deposited colorless solid was recovered by filtration, washed with cold hexane, and dried under vacuum to additionally obtain *N,N'*-*trans*-cyclohexane-1,2-diylbis(4-chlorobutanamide) (3.54 g, 25% yield). ¹H NMR revealed that both compounds prepared here were identical to each other. The total yield was 71%. ¹H NMR (δ /ppm vs. TMS, CDCl₃, 399.78 MHz) 5.58 (NH, bd, 2H), 3.94 (N–CH_{ax}, br, 2H), 3.62 (CH₂Cl, t, 4H), 2.36 (CH₂, t, 4H), 2.12 (CH₂, quintet, 4H), 1.77 (CH_{eq}, m, 4H), 1.57 (CH_{ax}, m, 4H). ¹³C NMR (δ /ppm vs. TMS, CDCl₃, 100.53 MHz) 170.98, 45.78, 44.69, 33.48, 28.37, 28.16.

This precursor (3.54 g, 11.0 mmol) was loaded in a 200 mL round bottom flask together with THF (110 mL), followed by cooling in the ice bath. To this solution, potassium *tert*-butoxide (2.57 g, 22.9 mmol) dissolved in THF (30 mL) was slowly added through a dropping funnel. The reaction mixture was stirred at 0 °C for 1 h and further reacted at room temperature for 6 h. After passing through a Celite pad, the filtrate was concentrated by a rotary evaporator. The residue was mixed with CH₂Cl₂ (80 mL) and 1 M HCl aq (10 mL), followed by stirring for several minutes. The separated organic layer was mixed with K₂CO₃ and MgSO₄. After removal of the solid residues, the filtrate was evaporated under reduced pressure to dryness to obtain a colorless microcrystalline compound of *rac*-L2 (2.46 g) at a 90% yield. ¹H NMR (δ /ppm vs. TMS, CDCl₃, 399.78 MHz) 4.04 (N–CH_{ax}, br, 2H), 3.51 (CH₂, t, 4H), 2.39 (CH₂, t, 4H), 2.03 (CH₂, quintet, 4H), 1.87 (CH_{eq}, m, 4H), 1.730 (CH_{ax}, m, 4H). ¹³C NMR (δ /ppm vs. TMS, CDCl₃, 100.53 MHz) 175.02, 48.02, 45.73, 31.42, 27.18, 18.42.

4.4. Synthesis of [Np^{VI}O₂(NO₃)₂(L1)]_n

A stock solution of 100 mM Np^{VI}O₂²⁺ in 3 M HNO₃ (25 μ L), a blank 3 M HNO₃(aq) (50 μ L), and a stock solution of 200 mM L1 in 3 M HNO₃(aq) were layered from bottom to top of a glass tube (*ca.* ϕ 5 mm diameter) in a stepwise manner, followed by standing in a silent place in the glovebox at 293 K. After one day passed, brown block crystals of [Np^{VI}O₂(NO₃)₂(L1)]_n were obtained at 44% yield, which was estimated by the following procedure. The supernatant (1 μ L) was loaded into a *ca.* ϕ 10 mm glass vial and subjected to γ -ray spectrometry, performed at VKTA Dresden. The γ -ray emission from the sample was counted for 25 min real time plus 0.71% dead time.

4.5. Crystallographic Analysis

The X-ray diffraction data of the well-shaped single crystal of [Np^{VI}O₂(NO₃)₂(L1)]_n were collected by the Bruker D8 VENTURE diffractometer equipped with hybrid pixel array detector and graphite monochromated Mo K α radiation (λ = 0.71073 Å). A selected single crystal of the sample was mounted on a MiTeGen Dual Thickness MicroMounts with mineral oil. Intensity data were collected by taking oscillation photographs. Reflection data were integrated with the Bruker SAINT software package. Absorption correction was applied using the strong absorber option of SADAS22. The structures were solved by the direct method and refined anisotropically for non-hydrogen atoms by full-matrix least-squares calculations with the SHELX program suite [27]. Each refinement was continued until all shifts were smaller than one-third of the standard deviations of the parameters involved. Hydrogen atoms were located at the calculated positions. All hydrogen atoms were constrained to an ideal geometry with C–H = 0.95 Å. The thermal parameters of all hydrogen atoms were related to those of their parent atoms by $U(\text{H}) = 1.2U_{\text{eq}}(\text{C})$. All calculations were performed using the Olex2 crystallographic software program package [28].

The crystallographic data of $[\text{NpO}_2(\text{NO}_3)_2(\text{L1})]_n$ are summarized in Table 1 together with those of $[\text{UO}_2(\text{NO}_3)_2(\text{L1})]_n$, which we reported previously [9].

Supplementary Materials: The following supporting information can be downloaded at <https://www.mdpi.com/article/10.3390/inorganics11030104/s1>. Figure S1: Packing diagram of $[\text{NpO}_2(\text{NO}_3)_2(\text{L1})]_n$; Table S1: Logarithmic stability constants ($\log \beta$) of typical actinyl(VI) complexes ($\text{AnO}_2(\text{L})_n^{m+}$; An = U, Np, Pu; L = CO_3^{2-} , CH_3COO^- , F^- , Cl^- , NO_3^- , SO_4^{2-}), in aqueous systems at 298 K and zero ionic strength; and references cited therein.

Author Contributions: T.T.: Conceptualization, Data curation, Formal analysis, Investigation, Funding acquisition, Project administration, Writing—original draft. J.M.: Conceptualization, Methodology, Resources, Formal analysis, Investigation, Writing—review and editing. R.O.: Conceptualization, Investigation, Funding acquisition, Project administration, Writing—review and editing. S.T.: Conceptualization, Investigation, Funding acquisition, Project administration, Writing—review and editing. K.T.: Conceptualization, Data curation, Formal analysis, Funding acquisition, Investigation, Project administration, Supervision, Writing—original draft, Writing—review and editing. All authors have read and agreed to the published version of the manuscript.

Funding: This work was partly supported by JSPS KAKENHI (No. JP20KK0119 to S.T., JP21J11942 to T.T., JP22J23423 to R.O.) and JSPS Overseas Challenge Program for Young Researchers (No. JP202280007 to T.T.).

Data Availability Statement: CCDC 2208277 contains the supplementary crystallographic data for this paper. These data can be obtained free of charge via www.ccdc.cam.ac.uk/data_request/cif (accessed on 24 February 2023), or by emailing data_request@ccdc.cam.ac.uk, or by contacting The Cambridge Crystallographic Data Centre, 12 Union Road, Cambridge CB2 1EZ, UK; Fax: +44-1223-336033.

Acknowledgments: We thank Stephan Weiß (HZDR) for their technical assistance related to γ -ray spectrometry.

Conflicts of Interest: The authors declare no conflict of interest.

References

1. Benedict, M.; Pigford, T.H.; Levi, H.W. *Nuclear Chemical Engineering*, 2nd ed.; McGraw-Hill: New York, NY, USA, 1981.
2. Takao, K.; Ikeda, Y. Coordination Chemistry of Actinide Nitrates with Cyclic Amide Derivatives for the Development of the Nuclear Fuel Materials Selective Precipitation (NUMAP) Reprocessing Method. *Eur. J. Inorg. Chem.* **2020**, *2020*, 3443–3459. [[CrossRef](#)]
3. Kim, S.-Y.; Takao, K.; Haga, Y.; Yamamoto, E.; Kawata, Y.; Morita, Y.; Nishimura, K.; Ikeda, Y. Molecular and Crystal Structures of Plutonyl(VI) Nitrate Complexes with *N*-Alkylated 2-Pyrrolidone Derivatives: Cocrystallization Potentiality of U^{VI} and Pu^{VI} . *Cryst. Growth Des.* **2010**, *10*, 2033–2036. [[CrossRef](#)]
4. Morita, Y.; Kawata, Y.; Mineo, H.; Koshino, N.; Asanuma, N.; Ikeda, Y.; Yamasaki, K.; Chikazawa, T.; Tamaki, Y.; Kikuchi, T. A Study on Precipitation Behavior of Plutonium and Other Transuranium Elements with *N*-Cyclohexyl-2-pyrrolidone for Development of a Simple Reprocessing Process. *J. Nucl. Sci. Technol.* **2007**, *44*, 354–360. [[CrossRef](#)]
5. Loubert, G.; Henry, N.; Volkringer, C.; Duval, S.; Tamain, C.; Arab-Chapelet, B.; Delahaye, T.; Loiseau, T. Quantitative Precipitation of Uranyl or Plutonyl Nitrate with *N*-(1-Adamantyl)acetamide in Nitric Acid Aqueous Solution. *Inorg. Chem.* **2020**, *59*, 11459–11468. [[CrossRef](#)] [[PubMed](#)]
6. Vats, B.G.; Bhattacharyya, A.; Sanyal, K.; Kumar, M.; Gamare, J.S.; Kannan, S. Piperazinyl-Based Diamide Ligand for Selective Precipitation of Actinyl ($\text{UO}_2^{2+}/\text{PuO}_2^{2+}$) Ions with Fast Kinetics. *Inorg. Chem.* **2021**, *60*, 17529–17536. [[CrossRef](#)]
7. Morss, L.R.; Edelstein, N.M.; Fuger, J. *The Chemistry of the Actinide and Transactinide Elements*, 4th ed.; Springer: Dordrecht, The Netherlands, 2011.
8. Takao, K.; Ikeda, Y.; Kazama, H. New concept for molecular design of *N*-substituted 2-pyrrolidone derivatives towards advanced reprocessing method for spent ThO_2 fuels. *Ener. Proc.* **2017**, *131*, 157–162. [[CrossRef](#)]
9. Kazama, H.; Tsushima, S.; Ikeda, Y.; Takao, K. Molecular and Crystal Structures of Uranyl Nitrate Coordination Polymers with Double-Headed 2-Pyrrolidone Derivatives. *Inorg. Chem.* **2017**, *56*, 13530–13534. [[CrossRef](#)]
10. Kazama, H.; Takao, K. Molecular Design of Double-headed 2-Pyrrolidone Derivatives for Separation/Co-precipitation of UO_2^{2+} from/with Tetravalent Actinides towards Nuclear Fuel Recycling. *Chem. Lett.* **2020**, *49*, 1201–1205. [[CrossRef](#)]
11. Koshino, N.; Harada, M.; Morita, Y.; Kikuchi, T.; Ikeda, Y. Development of a simple reprocessing process using selective precipitant for uranyl ions: Fundamental studies for evaluating the precipitant performance. *Prog. Nucl. Energy* **2005**, *47*, 406–413. [[CrossRef](#)]

12. Takao, K.; Noda, K.; Morita, Y.; Nishimura, K.; Ikeda, Y. Molecular and Crystal Structures of Uranyl Nitrate Complexes with *N*-Alkylated 2-Pyrrolidone Derivatives: Design and Optimization of Promising Precipitant for Uranyl Ion. *Cryst. Growth Des.* **2008**, *8*, 2364–2376. [CrossRef]
13. Takao, K.; Noda, K.; Nogami, M.; Sugiyama, Y.; Harada, M.; Morita, Y.; Nishimura, K.; Ikeda, Y. Solubility of Uranyl Nitrate Precipitates with *N*-Alkyl-2-pyrrolidone Derivatives (Alkyl = *n*-Propyl, *n*-Butyl, *iso*-Butyl, and Cyclohexyl). *J. Nucl. Sci. Technol.* **2009**, *46*, 995–999. [CrossRef]
14. Inoue, T.; Kazama, H.; Tsushima, S.; Takao, K. Essential Role of Heterocyclic Structure of *N*-Alkylated 2-Pyrrolidone Derivatives for Recycling Uranium from Spent Nuclear Fuels. *Bull. Chem. Soc. Jpn.* **2020**, *93*, 846–853. [CrossRef]
15. Fuger, J.; Spahiu, K.; Sullivan, J.C.; Nitsche, H.; Ullman, W.J.; Potter, P.; Vitorge, P.; Rand, M.H.; Wanner, H.; Rydberg, J. *Chemical Thermodynamics of Neptunium and Plutonium*; Elsevier Science B. V.: Amsterdam, The Netherlands, 2001.
16. Grenthe, I.; Gaona, X.; Plyasunov, A.V.; Rao, L.; Runde, W.H.; Grambow, B.; Konings, R.J.M.; Smith, A.L.; Moore, E.E. *Second Update on the Chemical Thermodynamics of Uranium, Neptunium, Plutonium, Americium and Technetium*; OECD Nuclear Energy Agency, Data Bank: Paris, France, 2020.
17. Casellato, U.; Vigato, P.A.; Vidali, M. Actinide nitrate complexes. *Coord. Chem. Rev.* **1981**, *36*, 183–265. [CrossRef]
18. Jones, M.B.; Gaunt, A.J. Recent developments in synthesis and structural chemistry of nonaqueous actinide complexes. *Chem. Rev.* **2013**, *113*, 1137–1198. [CrossRef] [PubMed]
19. Alcock, N.W.; Roberts, M.M.; Brown, D. Actinide structural studies. Part 1. Crystal and molecular structures of dinitratodioxo-bis(triphenylphosphine oxide)neptunium(VI), dinitratodioxo-bis(triphenylphosphine oxide)uranium(VI), and dichlorodioxo-(triphenylphosphine oxide)neptunium(VI). *J. Chem. Soc. Dalton Trans.* **1982**, 25–31. [CrossRef]
20. Alcock, N.W.; Flanders, D.J.; Brown, D. Actinide structural studies. Part 7. The crystal and molecular structures of (2,2'-bipyridyl)dinitratodioxo-uranium(VI) and -neptunium(VI), and diacetato-(2,2'-bipyridyl)dioxo-uranium(VI) and -neptunium(VI). *J. Chem. Soc. Dalton Trans.* **1985**, 1001–1007. [CrossRef]
21. Uhanov, A.S.; Sokolova, M.N.; Fedoseev, A.M.; Bessonov, A.A.; Nechaeva, O.N.; Savchenkov, A.V.; Pushkin, D.V. New Complexes of Actinides with Monobromoacetate Ions: Synthesis and Structures. *ACS Omega* **2021**, *6*, 21485–21490. [CrossRef]
22. Autillo, M.; Wilson, R.E. Molecular Hydroxo-Bridged Dimers of Uranium(VI), Neptunium(VI), and Plutonium(VI): [Me₄N]₂[(AnO₂)₂(OH)₂(NO₃)₄]. *Inorg. Chem.* **2019**, *58*, 3203–3210. [CrossRef]
23. Charushnikova, I.A.; Grigor'ev, M.S.; Fedoseev, A.M. Nitrate Complexes of Neptunium(V) with Organic Single-Charged Cations in the Outer Sphere. *Radiochemistry* **2020**, *62*, 301–307. [CrossRef]
24. Smith, R.M.; Martell, A.E.; Motekaitis, R.J. NIST Critically Selected Stability Constants of Metal Complexes Database. Volume Ver. 8.0. 2004. Available online: <https://data.nist.gov/od/id/mds2-2154> (accessed on 25 February 2023).
25. Takao, K.; Kazama, H.; Ikeda, Y.; Tsushima, S. Crystal Structure of Regularly *T_h*-Symmetric [U(NO₃)₆]²⁻ Salts with Hydrogen Bond Polymers of Diamide Building Blocks. *Angew. Chem. Int. Ed.* **2019**, *58*, 240–243. [CrossRef]
26. Takao, K.; März, J.; Matsuoka, M.; Mashita, T.; Kazama, H.; Tsushima, S. Crystallization of colourless hexanitratoneptunate(IV) with anhydrous H⁺ counteranions trapped in a hydrogen bonded polymer with diamide linkers. *RSC Adv.* **2020**, *10*, 6082–6087. [CrossRef] [PubMed]
27. Sheldrick, G.M. Crystal structure refinement with SHELXL. *Acta Crystallogr.* **2015**, *C71*, 3–8. [CrossRef]
28. Dolomanov, O.V.; Bourhis, L.J.; Gildea, R.J.; Howard, J.A.K.; Puschmann, H. OLEX2: A complete structure solution, refinement and analysis program. *J. Appl. Crystallogr.* **2009**, *42*, 339–341. [CrossRef]

Disclaimer/Publisher's Note: The statements, opinions and data contained in all publications are solely those of the individual author(s) and contributor(s) and not of MDPI and/or the editor(s). MDPI and/or the editor(s) disclaim responsibility for any injury to people or property resulting from any ideas, methods, instructions or products referred to in the content.